

1
2
3
4
5
6
7
8
9
10
11
12
13
14
15
16
17
18
19
20
21
22
23
24
25
26

Received Date : 02-Sep-2016

Revised Date : 29-Nov-2016

Accepted Date : 29-Nov-2016

Article type : JAM - Original Article

The Effect of Inoculum Source and Fluid Shear Force on the Development of *In Vitro* Oral Multi-species Biofilms

Constanza E. Fernández^{1,2}, Marcelo B. Aspiras³, Michael W. Dodds³, Carlos González-Cabezas², Alexander H. Rickard^{1*}

¹ Department of Epidemiology, School of Public Health, University of Michigan, Ann Arbor, MI, USA.

² Department of Cariology, Restorative Sciences and Endodontics, School of Dentistry, University of Michigan, Ann Arbor, MI, USA.

³ Scientific Discovery, Global Innovation Center (GIC), Wrigley, Chicago, IL, USA.

Running title: *In Vitro* Oral Biofilm Development

Numbers of Figures: 5

This is the author manuscript accepted for publication and has undergone full peer review but has not been through the copyediting, typesetting, pagination and proofreading process, which may lead to differences between this version and the [Version of Record](#). Please cite this article as [doi: 10.1111/jam.13376](https://doi.org/10.1111/jam.13376)

This article is protected by copyright. All rights reserved

27 Numbers of Tables: 1

28

29

30 * **Correspondent author:**

31 Alexander H. Rickard.

32 School of Public Health, Department of Epidemiology, University of Michigan

33 1415 Washington Heights, Ann Arbor, MI 48109-1078, USA

34 Phone: 734-616-8491

35 E-mail: alexhr@umich.edu

36 **Abstract**

37 **Aim:** Saliva has been previously used as an inoculum for *in-vitro* oral biofilm
38 studies. However, the microbial community profile of saliva is markedly
39 different from hard and soft tissue-associated oral biofilms. Here, we
40 investigated the changes in the biofilm architecture and microbial diversity of
41 *in-vitro* oral biofilms developed from saliva, tongue or plaque-derived inocula
42 under different salivary shear forces. **Methods and Results:** Four inoculum-
43 types (saliva, bacteria harvested from the tongue, toothbrush and curette-
44 harvested plaque) were collected and pooled. Biofilms ($n \geq 15$) were grown
45 for 20 h in cell-free human saliva flowing at three different shear forces.
46 Stained biofilms were imaged using a confocal laser scanning microscope.
47 Biomass, thickness and roughness were determined by image analysis and
48 bacterial community composition analyzed using Ion Torrent. All developed
49 biofilms showed a significant reduction in observed diversity compared to
50 their respective original inoculum. Shear force altered biofilm architecture of
51 saliva and curette-collected plaque and community composition of saliva,
52 tongue and curette-harvested plaque. **Conclusions:** Different intraoral
53 inocula served as precursors of *in-vitro* oral polymicrobial biofilms which can
54 be influenced by shear. **Significance and Impact of the Study:** Inoculum
55 selection and shear force are key factors to consider when developing multi-
56 species biofilms within *in-vitro* models.

57

58 **Keywords:** Confocal laser scanning microscopy, saliva, dental plaque,
59 tongue, biodiversity, microbiome, bacteria, 16S rRNA

60 **Introduction**

61
62 Oral biofilms are architecturally and taxonomically complex microbial
63 communities that develop on teeth to form visually conspicuous dental
64 plaque (Nyvad & Fejerskov, 1987, Mark Welch, *et al.*, 2016). Oral biofilms
65 can contain hundreds of species of bacteria (Dewhirst, *et al.*, 2010). These
66 biofilm communities develop through tightly orchestrated cell-cell
67 interactions (Rickard, *et al.*, 2003, Hojo, *et al.*, 2009) and their formation is
68 influenced by the colonizing species, the prevailing environmental conditions,
69 and the topographical and physicochemical properties of the surface to
70 which the colonizing bacteria adhere (Song, *et al.*, 2015). Through cell-cell
71 and cell-environment interactions, which influence the species composition
72 and architecture, oral biofilms can develop to cause caries and periodontal
73 diseases (Jakubovics & Kolenbrander, 2010). The multi-species composition
74 and the biofilm-specific lifestyle of the component bacteria are responsible
75 for the recalcitrance of biofilms to physical and chemical control strategies
76 (Gilbert, *et al.*, 2002, Marsh, 2003, ten Cate & Zaura, 2012).

77
78 *In vitro* model biofilm systems are commonly used to gain knowledge of
79 changes in biofilm architecture and composition, especially when trying to
80 understand the development of disease-causing biofilms and when
81 evaluating the effectiveness of antimicrobial/anti-biofilm compounds
82 (Kinniment, *et al.*, 1996, McBain, 2009, Zijngel, *et al.*, 2012, Salli &
83 Ouwehand, 2015). However, many *in vitro* model systems are arguably not
84 particularly representative of the conditions within the human oral cavity
85 (McBain, 2009, Coenye & Nelis, 2010). Such a potential lack of
86 representation is typically due to the use of artificial medium and/or the use
87 of one or a few strains of bacteria (Saunders & Greenman, 2000,
88 Guggenheim, *et al.*, 2001, Fernández, *et al.*, 2016). Given the bacterial

89 diversity of human oral biofilms, it would conceivably be preferable to use
90 natural inocula to facilitate the development of *in vitro* biofilms to more
91 broadly represent the *in vivo* community (Burmolle, *et al.*, 2014, Kistler, *et*
92 *al.*, 2015). Recently, we developed an *in vitro* microfluidic oral biofilm
93 system that uses filter-sterilized 25% pooled human saliva as the medium
94 and pooled human saliva as the inoculum (Nance, *et al.*, 2013, Samarian, *et*
95 *al.*, 2014, Kolderman, *et al.*, 2015). Using confocal laser scanning
96 microscopy (CLSM), multi-species biofilms were shown to be architecturally
97 complex and containing predominantly viable cells. The multi-species
98 biofilms, also referred herein as polymicrobial biofilms, that formed within
99 the system also contained species that are typically identified within *in vivo*
100 supragingival dental plaque biofilms (Nance, *et al.*, 2013). This included
101 species that are often regarded as being highly refractory to cultivation,
102 including members of the candidate division TM7 (Soro, *et al.*, 2014, He, *et*
103 *al.*, 2015). However, as opposed to our *in vitro* model system, the human
104 oral cavity is composed of numerous surface-types, exposed to different
105 environmental conditions and subject to colonization by different species in a
106 site-dependent (and niche-dependent) manner (Aas, *et al.*, 2005). Cognizant
107 of the anatomical and environmental diversity of the human oral cavity, we
108 hypothesized that inocula derived from biofilms at different sites would give
109 rise to taxonomically and architecturally distinct biofilms in our *in vitro*
110 model system. Given that salivary flow also varies between sites *in vivo*, we
111 hypothesized that shear might alter the architectural and taxonomic
112 characteristics of the biofilms.

113

114 The aim of this study was to characterize differences in the biofilm
115 architecture and microbial biofilm diversity of *in vitro* microfluidic-grown
116 biofilms developed from saliva, tongue or plaque-derived inocula under
117 different fluid shear. Findings from this study indicate that the architecture
118 and biofilm community composition of developed *in vitro* oral biofilms is
119 influenced by the source and harvesting approach to acquire inocula for this

120 *in vitro* model system. Furthermore, evidence suggested that salivary shear
121 influenced the architecture and community composition/diversity of the
122 biofilms in an inoculum-dependent manner.

123

124 **Materials and Methods**

125

126 ***Summary of Experimental Design***

127 Saliva samples, bacteria harvested from the tongue, toothbrush-harvested
128 plaque and curette-harvested plaque were collected from four healthy
129 donors and pooled to make four inoculum-types, based upon the source
130 from which they were harvested. Biofilms from these four inoculum-types
131 were grown in cell free human saliva (CFS) in 24-channel Bioflux™
132 microfluidic plates for 20 h. CFS was flowed through the system at 0.1, 0.2
133 or 0.4 dyn cm⁻² (fluid shear force) to yield a total of twelve experimental
134 groups (four inoculum-types at three fluid shear forces). Developed biofilms
135 were labeled with a vitality stain and imaged using a confocal laser scanning
136 microscope. Biomass, thickness and roughness were calculated from the
137 collected images. Experiments were performed in at least three independent
138 assays (i.e. across three microfluidic plates). In each assay, between four to
139 six channels supported biofilm growth from each experimental group. This
140 facilitated the analysis of a total of 15 to 17 channels per group across three
141 independent assays (i.e. n=15-17). For each channel, three CLSM images
142 were taken for analysis. For each experimental group, developed biofilms
143 from three channels were harvested in order to assess community
144 composition. Initial inocula (n=3 per inoculum-type) and developed biofilms
145 (n=3 per inoculum-type) were sequenced with Ion Torrent PGM™ platform.
146 Sequencing data were used to estimate alpha and beta diversity. The
147 architectural measures and community composition of the biofilms were
148 statistically compared considering fluid shear force and inoculum-type from
149 which they were derived.

150

151 **Patient Sampling**

152 This study was approved by the University of Michigan Institutional Review
153 Board for Human Subject Research (ID# HUM00101254). Samples were
154 collected from four consenting healthy donors, who did not have any known
155 underlying chronic disease and in good oral health. The donors had not
156 received antibiotics for at least three months prior to collection. Collection of
157 samples was performed in the morning for all volunteers. They were asked
158 to refrain from ingesting food and brushing their teeth the morning of the
159 collection.

160
161 To generate a saliva-inoculum, stimulated saliva was collected during
162 mastication of parafilm until 5 mL was collected in a sterile plastic tub. To
163 generate a tongue-inoculum, a sterile stainless steel tongue cleaner was
164 drawn firmly over the dorsum of the tongue until all visible material had
165 been removed. All the fluid collected was deposited in a sterile plastic tube.
166 To generate a toothbrush-plaque-inoculum plaque was removed using a
167 toothbrush. For this, donors were shown how to perform vertical movements
168 in all the buccal and lingual surfaces for a total of two minutes. The plaque
169 removed and the saliva accumulated in the mouth were collected in a sterile
170 plastic tube. To generate the curette-harvested plaque-inoculum, visible
171 accumulated plaque on dental surfaces was removed using a sterile curette.
172 During sampling, plaque was collected in a sterile tube containing 500 μL of
173 pre-reduced 10 mmol l^{-1} sodium phosphate buffer (pH 8.0) (Shu, *et al.*,
174 2007). Samples of each inoculum-type from the different donors were
175 pooled, filtered using a 70 μm nylon filter to remove organic residual and
176 glycerol was added to form a mixture containing a final concentration of
177 25% glycerol. Samples were stored in individual aliquots at -80°C until
178 required.

179
180 Cell-free pooled human saliva (CFS) was used as a natural nutrient source to
181 mimic *in vivo* conditions inside the microfluidic biofilm model (Nance, *et al.*,

182 2013, Samarian, *et al.*, 2014). For this, around 30 ml stimulated saliva was
183 collected from the same donors. The saliva was pooled and dithiothreitol was
184 added at 2.5 mmol l⁻¹ to prevent protein agglomeration. In order to remove
185 visible particulate material, the pooled saliva was centrifuged for 30 min at
186 17,500 g. The resulting particulate-free saliva was diluted to 25% using
187 deionized water and filter sterilized (0.22 µm polyethersulfone filter).
188 Individual aliquots were stored at -80°C until use.

189

190

191

192 ***Microfluidic Biofilm Model System***

193 Biofilms were grown in a 24-channel Bioflux™ microfluidic system (Fluxion,
194 South San Francisco, CA, USA) as described by Samarian et al., (2014). This
195 model system contains 24 channels (6 mm long, 350 µm wide, 70 µm high)
196 which are individually connected to an inlet- and outlet-well. Biofilms
197 develop on the glass surfaces within the channels which are exposed
198 continuously to growth medium (ie. CFS) flowing at a defined shear forces.
199 Briefly, CFS was used to coat the channels of the microfluidic system for 20
200 min to simulate acquired pellicle formation. Each channel was subsequently
201 inoculated with one of the four inoculum types (saliva samples, bacteria
202 harvested from the tongue, toothbrush-harvested plaque and curette-
203 harvested plaque) and incubated for 45 min at 37°C. CFS was flowed in the
204 system at 0.1, 0.2 or 0.4 dyn cm⁻² (fluid shear force) during 20 h at 37°C
205 under aerobic conditions (i.e., saliva was not pre-reduced).

206

207 ***Biofilm Staining, Imaging, and Analysis.***

208 After 20 h growth, developed biofilms were washed with PBS (pH 7.4) at 0.2
209 dyn cm⁻² for 20 min. Live/Dead® reagent (Invitrogen, CA, USA) was diluted
210 in PBS to contain 10 µmol l⁻¹ SYTO 9 and 60 µmol l⁻¹ propidium iodide,

211 introduced into the channels at 0.2 dyn cm^{-2} , and allowed to stain the
212 biofilms for 45 min at room temperature. Subsequently, the biofilms were
213 washed for 20 min with PBS to remove excess stain from the channels.

214 Three random representative image stacks were taken of the developed
215 biofilm per channel using an inverted Leica SPE CLSM (Leica, Exton, PA,
216 USA) equipped with a HCX PL APO 40X/0.85 CORR CS dry microscope
217 objective (Leica, Exton, PA, USA). IMARIS Version 7.3.1 software (Bitplane,
218 Zurich, Switzerland) was used to render images in 3D by using the *Surpass*
219 visualization software component. Biomass, average thickness and
220 roughness were calculated using COMSTAT2 software (Heydorn, *et al.*,
221 2000). Using the approach of Nance and colleagues (Nance *et al.*, 2013), cell
222 viability was calculated by determining the percentage of green pixels (from
223 the total of green and red pixels) in each image stack using ImageJ software
224 (Collins, 2007). All renderings and quantification analyses were performed
225 on a PC equipped with Radeon 5850 1 Gb graphics card (AMD, Sunnyvale,
226 CA, USA). Generated renderings were assembled in CorelDRAW v. X5 (Corel,
227 Mountain View, CA, USA).

228

229 ***Harvesting of Samples and Genomic Analysis***

230 Three channels from three different microfluidic plates (i.e. representing
231 independent experiments) were randomly selected to harvest the developed
232 biofilms. To perform this, the outlet-well was washed three times with sterile
233 deionized water and all solution inside the inlet and outlet well completely
234 removed. Following the washing step, 100 μL sterile deionized water was
235 flowed through the channel that contained the biofilm at 20 dyn cm^{-2} in
236 forward and reverse direction to remove the attached biofilm as described by
237 Samarian *et al.* (2013).

238

239 DNA was extracted from harvested biofilms using DNeasy Blood & Tissue Kit
240 (Qiagen, Hilden, Germany). An automated standard protocol was used in

241 concert with the QIACUBE (Qiagen, Hilden, Germany) to extract DNA
242 reducing technical variation prior to sequencing. PCR primers for the V4
243 variable region (515-806) of the 16S rRNA gene were amplified in a single-
244 step 30 cycle PCR using a HotStarTaq Plus Master Mix Kit (Qiagen, Valencia,
245 CA, USA). This was performed using the following conditions: 94°C for 3
246 min, followed by 28 cycles at 94°C for 30 s, 53°C for 40 s and 72°C for 1
247 min, with a final elongation step at 72°C for 5 min. Sequencing was carried-
248 out at MR DNA (www.mrdnlab.com, Shallowater, TX, USA) using an Ion
249 Torrent™ PGM and following the manufacturer's instructions (Thermo Fisher
250 Scientific, Waltham, MA USA).

251
252 Raw sequences were processed in-house with QIIME (ver. 1.9.0). Sequences
253 with ambiguous base calls, an average Phred quality score below 25,
254 homopolymer length of >6, primer mismatch exceeding 0, or read length
255 that is below 200 bp were discarded. All sequences that remained after this
256 filtering step, had primers, adaptors, and linker sequences truncated.
257 Operational taxonomic units (OTUs) were clustered by 97% identity using an
258 open-referenced OTU picking strategy with PyNAST sequence aligner against
259 the CORE database (Caporaso, *et al.*, 2010a, Griffen, *et al.*, 2011).
260 Taxonomy was assigned using the RDP Classifier (Wang, *et al.*, 2007) in
261 QIIME. Singleton OTUs were filtered out as part of the default QIIME
262 parameters. Additionally, OTUs constituting less than .05% of total reads
263 were filtered out. The final OTU table was analyzed with QIIME (Caporaso, *et*
264 *al.*, 2010b) and the Phyloseq package in R (McMurdie & Holmes, 2013).
265 Downstream analytics include Shannon-Weaver within-sample diversity,
266 community relative abundance, and unweighted UniFrac distances between
267 samples. Outcomes were measured within the Phyloseq package and
268 graphical output generated with R's ggplot package. For principal
269 coordinates construction, the jackknifed_beta_diversity.py pipeline within
270 QIIME was used.

271

272 **Statistical Analysis.**

273 Statistical analyses were performed using R (RStudio, Inc.,
274 version 0.99.489) for beta diversity and SPSS (IBM Corp., version 23.0,
275 Armonk, NY, USA) for architecture outcomes and alpha diversity. For
276 biomass and thickness differences among groups were analyzed using
277 ANOVA/ Tukey's test. Biofilm roughness and Shannon-Weaver alpha
278 diversity differences were tested using Kruskal-Wallis/Mann-Whitney. The
279 effect of shear was also analyzed using a linear regression analysis. The
280 significance threshold was set at .05 for all analyses.

281

282

283 **Results**

284

285 **Architectural Properties of Biofilms Developed from Different**
286 **Inoculum-Types**

287 Each inoculum type developed architecturally complex biofilms under the
288 three different shear forces. Representative images of these developed
289 biofilms are presented in Figure 1. As inferred by the Live/Dead stain, by
290 determining the ratio of red to green cells, the amount of viable (green
291 fluorescently labeled) cells predominated over the damaged/dead (red
292 fluorescently labeled) cells (Fig. 1). The average green fluorescence was
293 always >75% for the biofilms developed from each inoculum and under each
294 shear force ($90.35 \pm 9.31\%$ of viability; average \pm SD; n=187 channels).
295 While no unique architectural structures could be assigned to either the
296 inoculum from which the biofilm was developed or the shear force applied, it
297 was evident that the biofilms that were developed from the toothbrush- and
298 curette-developed plaque biofilms were generally more homogenous in
299 structure (i.e. lacking larger biofilm biomasses) and consisted of many small
300 biofilm micro colonies, as compared to biofilms developed from saliva and
301 tongue inoculums.

302 Of note, image analysis showed that different shear forces (0.1, 0.2 and 0.4
303 dyn cm^{-2}) exhibited quantifiable significant differences ($p < 0.05$) to affect the
304 architectural properties (biomass, thickness, and roughness) of the saliva
305 and curette plaque developed biofilms. In particular, regression analysis
306 showed that increasing shear force, increased the biomass and thickness of
307 biofilms derived from the saliva and curette-plaque-developed biofilms (Fig.
308 2). Compared to biofilms developed at the lowest shear (0.1 dyn cm^{-2}), the
309 highest shear (0.4 dyn cm^{-2}) resulted in the development of two-fold thicker
310 biofilms from curette-harvested plaque and the development of three-fold
311 thicker biofilms from collected saliva. By analyzing the distribution of the
312 biomass and thickness values, biofilms developed under 0.2-dyn cm^{-2}
313 demonstrated the least variability in architectural outcomes (Fig. 2).
314 Although, considering the large standard deviation of values of biomass and
315 thickness, saliva-derived biofilms were also the most architecturally variable
316 biofilms. Differences by shear force were only observed in roughness values
317 for biofilms developed from saliva and tongue inocula, whereby increasing
318 the shear significantly reduced the roughness values (Supporting
319 Information: Table S1). Toothbrush-plaque and tongue were seemingly the
320 least responsive to shear, showing very little change in architecture, except
321 for roughness for biofilms developed from the pooled tongue inoculum.

322
323 It was observed that only biofilms developed at 0.2 dyn cm^{-2} exhibited
324 significant architectural differences among inocula (Fig. 2 and Supporting
325 Information: Table S1). At this shear, biomass and thickness of biofilms
326 developed from saliva were greater and statistically different than curette-
327 plaque-developed biofilm ($p < 0.05$), while toothbrush-plaque-developed
328 biofilm was not statistically different to saliva and curette-plaque-developed
329 biofilm. For biofilms developed from tongue inocula, only the biofilm biomass
330 was significantly different to biofilms grown from saliva inocula (Supporting
331 Information: Table S1). No significant differences in biofilm roughness were
332 evident among inocula.

334 **Community Composition Analysis**

335 The most abundant genera in all our samples (pooled inocula and the
336 respective biofilms that developed from the inocula) were those typically
337 associated with the human oral microbiome and included *Streptococcus*,
338 *Neisseria*, *Rothia*, *Fusobacterium* and *Veillonella*. For the pooled plaque
339 inoculum and the biofilms developed from it, a large number of genera could
340 not be assigned to a taxonomic group (Supporting Information: Figure S1).
341 These unclassified genera belonged to a variety of families including
342 *Neisseriaceae*, *Streptococcaceae*, *Actinomycetaceae*, *Aerococcaceae*,
343 *Lachnospiraceae*, *Gemellaceae*, *Enterobacteriaceae*. Given the level of
344 taxonomic resolution, the relative abundance at family level for each
345 inoculum-type and their respective developed biofilms grown at 0.1, 0.2 and
346 0.4 dyn cm⁻² were derived and are shown in Figure 3. At the family level
347 (Fig. 3), the biofilm composition varied depending upon inoculum type and
348 shear force applied (which was also reflected at the genus level, for those
349 which could be classified; Supporting Information: Figure S1). Of particular
350 note was that for all inocula, specific equally dominant bacterial families
351 were abundant in all the inocula. These included members of the
352 *Streptococcaceae*, *Neisseriaceae*, *Veillonellaceae*, *Micrococcaceae*, and
353 *Actinomycetaceae*. In addition to members of these dominant bacterial
354 families, curette-derived plaque inocula also contained an abundance of
355 members of the *Fusobacteriaceae*. Developed from each of the four inocula
356 types, biofilms communities with substantially altered ratios of family
357 members were developed (Figure 3). In particular, members of the
358 *Streptococcaceae* and *Neisseriaceae* dominated at the expense of the other
359 bacterial families. In order to further quantify and compare the differences
360 across each community, alpha and beta diversity were assessed.

361

362 **i. Alpha Diversity**

363 The alpha diversity, estimated by determining the Shannon-Weaver Index
364 for each inoculum and biofilm sample, showed that each type of inoculum
365 possessed the largest alpha diversity, compared to the biofilms that
366 developed from them (Fig. 4). For the different inocula, the curette-plaque
367 derived inoculum possessed the largest alpha diversity, followed by the
368 toothbrush-derived plaque inoculum, and the inocula derived from the
369 tongue and saliva. Also, the shear influenced the alpha diversity of some of
370 the biofilms (Fig. 4). Increasing the imposed shear to 0.4-dyn cm⁻²
371 decreased alpha diversity of saliva-developed biofilms. Conversely, for
372 biofilms derived from the pooled tongue inoculum, the lowest alpha diversity
373 was observed at the intermediate shear of 0.2 dyn cm⁻². This was different
374 when compared with biofilms developed at 0.1 dyn cm⁻², but not statistically
375 different with biofilms developed at 0.4 dyn cm⁻² (Fig. 4). Biofilms developed
376 from toothbrush-plaque derived inocula were unaffected by shear (p>0.05).
377 Curette-plaque-developed biofilms seemingly showed greater alpha diversity
378 when developed under 0.4-dyn cm⁻² but not statistically different with slower
379 run shears (p>0.05).

380

381 **ii. Beta Diversity**

382 The beta diversity analysis is presented graphically in Figure 5 as a principal
383 coordinate analysis (PCoA) plot. In the plot, each colored point represents a
384 sample and the distance between samples represent the differences in
385 community composition (membership and bacteria abundances) among
386 individual samples. Three inoculum and three biofilm samples from each
387 inoculum source (toothbrush-derived plaque, curette-derived plaque, saliva
388 and tongue) are plotted using a color-coordinated approach (Fig. 5). As
389 visibly noticeable in Figure 5 and shown quantitatively in Table 1, the
390 inoculum and biofilm samples clustered into groups according to the sites
391 from which they were harvested. Unifrac distance values presented in Table
392 1 show the magnitude of the differences in community composition among

393 the groups presented in Figure 5. Toothbrush-plaque and curette-plaque
394 inocula were close (0.191 Unifrac distance) reflecting similar community
395 composition, while saliva (0.301) and tongue (0.327) were more distant to
396 plaque-derived inocula but closer between them (0.209) (Table 1 and Fig. 5,
397 A). Developed biofilms were far removed from the original inoculum (Table
398 1), nevertheless, they remained clustered by inoculum type in the PC2
399 (vertical-axis) (Fig. 5, B). Of the four inoculum types, developed curette-
400 plaque biofilms were the most dissimilar from its initial inoculum (Table 1,
401 0.664; 0.662 and 0.709 for 0.1 -0.2 -0.4 dyn cm⁻²) and tongue the most
402 similar (Table 1, 0.504, 0.540 and 0.489 for 0.1 -0.2 -0.4 dyn cm⁻²). In
403 addition, developed biofilms derived from the same inoculum and exposed to
404 different shear forces were clearly clustering together (Fig. 5). Shear-
405 induced clustering was statistically significant for biofilms developed from
406 saliva and toothbrush-plaque (Table 1).

407

408 Discussion

409 Inocula harvested from different oral niches facilitated the
410 development of *in vitro* polymicrobial oral biofilms within a microfluidic
411 system. Even though the developed biofilms had a reduced diversity
412 compared to the original inoculum, different inocula facilitated the
413 development of relatively specific biofilms, as highlighted by the beta
414 diversity analyses (Fig. 5 and Table 1). Because the model simulates a
415 constant salivary flow, the effect of three different velocities to generate
416 different shear forces was also tested. Biofilm architecture (Fig. 1 and 2) and
417 microbial community composition (Fig. 3 to 5) were seemingly influenced by
418 shear in an inoculum-dependent manner. Such a role for shear and
419 inoculum-type in the development of oral multi-species biofilms has received
420 only limited attention to date (Saunders & Greenman, 2000, Signori, *et al.*,
421 2016).

422

423 Our findings support previous reports indicating that the community
424 composition of oral biofilms is site specific (Segata, *et al.*, 2012, Simon-
425 Soro, *et al.*, 2013b) and that each type of inoculum develops taxonomically
426 unique communities that exhibit some similarity to the communities from
427 the original *in vivo* sites (Rudney, *et al.*, 2012). In agreement with our
428 findings, other studies have illustrated the differences between saliva and
429 plaque inocula (Rudney, *et al.*, 2012, Simon-Soro, *et al.*, 2013b), and
430 showed that the microbial composition of saliva is more similar to the
431 composition of tongue than it is to dental plaque (Mager, *et al.*, 2003) (Fig.
432 5). Such a similarity could relate to the shear effects on the tongue and
433 subsequent seeding of biofilm associated cells into the saliva, as opposed to
434 less pronounced shear effects on tooth-associated dental plaque biofilms.

435
436 When considering the stimulated saliva inoculum used in this study, a
437 concern could be that the community composition could be different from
438 unstimulated saliva. Evidence indicates that the stimulation of saliva
439 production (e.g. chewing parafilm) likely increased the release of bacteria
440 (Dawes, *et al.*, 2001). Work by Simon-Soro and colleagues indicated that
441 differences in diversity between stimulated and unstimulated saliva can be
442 present. Although, in their study, differences between stimulated and
443 unstimulated were variable; whereby stimulated saliva showed a lower
444 diversity than unstimulated saliva in one individual, and the reverse
445 relationship was found in the other individual (Simon-Soro, *et al.*, 2013b).
446 Conversely, another study reported that the microbial profiles of
447 unstimulated and stimulated saliva samples collected from the same person
448 have comparable composition (Belstrom, *et al.*, 2016). Thus, we decided to
449 use stimulated saliva as surrogate of unstimulated saliva for our studies
450 (Belstrom, *et al.*, 2016). Since the inocula we used in our study may overlap
451 “niches” (e.g. toothbrush-harvested inoculum mixes saliva and supra-
452 gingival plaque), the samples for each inoculum type were collected on
453 different days over the period of a week. Human oral biofilms have been

454 shown to be stable over a week (Belstrom, *et al.*, 2016), so the different
455 composition observed among inocula are likely related to the oral site/niche
456 and not related to temporal differences.

457

458 Few studies focus on the potential to develop biofilm communities that
459 are representative of specific the sites in the human oral cavity. For caries
460 research the use of supra-gingival dental plaque has been indicated to be
461 ideal source of bacteria to develop *in vitro* microcosms, but its collection is
462 sometimes not practical since human volunteers, qualified clinicians, and
463 specific equipment are needed. Another complexity associated with growing
464 representative biofilms *in vitro* from dental plaque inoculum is the specific
465 collection site. Dental plaque composition is influenced by teeth localization
466 (upper/lower, anterior/posterior), site of accumulation (proximal, cervical,
467 occlusal) and also the mineral status of the teeth (sound/demineralized,
468 active/inactive) (Simon-Soro, *et al.*, 2013a, Simon-Soro, *et al.*, 2013b)
469 which generates a potentially large variation in community composition in
470 the *in vitro* developed biofilm, depending on the place of sampling. For this
471 reason, some studies use specific areas for collection (Reilly, *et al.*, 2014),
472 while others pooled samples from different locations (Shu, *et al.*, 2007) to
473 attempt to reduce variability. For this work, we compared four different
474 types of pooled inoculums; saliva, bacteria harvested from the tongue,
475 toothbrush-harvested plaque and curette-harvested plaque. Toothbrush-
476 plaque and curette-plaque developed biofilms had more consistent biomass
477 and thickness values (more homogenous data) than saliva and tongue-
478 developed biofilm (Figure 2). Saliva developed biofilms with the most
479 variable architecture outcomes. Regarding community composition, all
480 biofilms grown from the different inocula showed a reduction in diversity.
481 *Streptococcus* and *Neisseria* dominated within the *in vitro* developed
482 biofilms. The species identity of these two genera as well as members of
483 other genera in the oral biofilms was difficult to determine due to the low
484 resolution to identify taxonomic units at genus level. This was especially for

485 curette-plaque and toothbrush-plaque developed biofilms. Such a problem is
486 explained by the short read lengths that traverse through V4 region in the
487 16S rRNA gene.

488

489 While it was observed that all the developed biofilms exhibited a
490 reduction in diversity, the use of inocula harvested from oral sites, facilitated
491 the development of multi-species biofilms that contains bacteria typically
492 isolated in dental plaque (Dewhirst, *et al.*, 2010). Our findings indicate that
493 toothbrush-plaque-developed biofilms retained the greatest diversity, while
494 biofilms developed from curette-harvested plaque exhibited a substantial
495 reduction of diversity. Despite this reduction in diversity, the use of human
496 inocula to develop *in vitro* microcosms still can be considered more
497 representative than the use of single species (Ccahuana-Vásquez & Cury,
498 2010, Fernández, *et al.*, 2016) or a defined consortia of bacteria (Saunders
499 & Greenman, 2000, Guggenheim, *et al.*, 2001). Additionally, the community
500 composition of the developed-biofilms collected from different channels and
501 from different experiments remained similar as highlighted by the clustering
502 in the PCoA (Fig. 5). This indicated reproducibility of our *in vitro* model.
503 Although some variation in viability, as inferred by image analysis, was
504 observed between developed biofilms, the average percent of green
505 fluorescence was always >75% in all groups. Differences between some
506 groups within the upper 25% range were observed but such differences are
507 difficult to evaluate in regard to viability (especially in polymicrobial
508 communities) (Netuschil, *et al.*, 2014) and may be a consequence of
509 experimental variation. Using the same microfluidic model we have observed
510 that the shifts in green fluorescence are considerably greater after treatment
511 to antimicrobials (Nance *et al.*, 2013).

512

513 Changes in fluid shear have been shown to cause alterations in biofilm
514 morphology (Klapper, *et al.*, 2002, Stoodley, *et al.*, 2002), thickness
515 (Rittman, 1982) and diversity (Rickard, *et al.*, 2004). In addition to the

516 changes in physical aspects of the biofilm, fluid shear can impact the
517 production of exopolysaccharides, mass transfer, and influence
518 metabolic/genetic behaviors (Liu & Tay, 2001, Liu & Tay, 2002). Some of
519 these observations could also be explained by the effect of fluid flow
520 conditions on cell-cell signaling (quorum-sensing) (Kim, *et al.*, 2016). In our
521 system, shear force seemed to influence biofilm architecture and community
522 composition but the effect was not evident for all inoculum types. Biomass
523 and thickness increased when shear force was increased, but only in biofilms
524 formed from saliva and curette-plaque inocula (Fig. 2). We hypothesize that
525 shear force affects biofilm architecture and community composition by
526 favoring the initial and subsequent attachment/retention of some species
527 and by altering the substrate availability.

528
529 Developed biofilm communities contained species that were present in
530 the inoculums from which they were derived (Fig. 3). However, these
531 biofilms communities were altered with respect to which bacterial families
532 dominated, as compared to the inoculums from which they were developed.
533 A number of reasons could account for the expansion of certain bacterial
534 families at the expense of others. For example, as compared to planktonic
535 populations, biofilm communities are subject to differences in environmental
536 factors, such as pH, dissolved oxygen, and substrate availability which exert
537 a large effect on the composition of oral microcosms grown *in vitro* (Brown &
538 Gilbert, 1993, Marsh, 2009, Zaura, *et al.*, 2009). These differences will also
539 conceivably change in a spatiotemporal manner as the biofilms develop. In
540 our model, specifically, members of the *Streptococcaceae* and *Neisseriaceae*
541 were seemingly selected for within the biofilms and were consequently the
542 most abundant. At the genera level, our data showed that *Neisseria* was
543 more prevalent in saliva developed biofilms. This observation is in
544 agreement with previous *in vitro* biofilm models where *Neisseria* was the
545 predominant species in multi-species developed biofilms (Saunders &
546 Greenman, 2000, Nance, *et al.*, 2013, Kistler, *et al.*, 2015) and as part of

547 the healthy 'core microbiome' of the human oral cavity (Zaura, *et al.*, 2009).
548 Also, it has been observed previously within an *in situ* model, that
549 *Streptococcus* and *Neisseria* dominated in the early phase of biofilm
550 development (Wake, *et al.*, 2016). Given that our model system is aerobic,
551 aerobic bacterial and facultative aerobic species were expected to be
552 common biofilm members. Future studies could explore the effect of
553 anaerobic conditions and longer periods to evaluate shifts in community
554 composition.

555
556 In conclusion, within a saliva-based *in vitro* model, different intraoral inocula
557 serve as precursors of oral biofilms. The biofilms developed in the model had
558 reduced bacterial diversity compared to the original inocula. Our data
559 indicates that inoculum selection and hydrodynamic shear force can
560 influence biofilm architecture and community composition. Thus, inoculum
561 type and shear are key factors to carefully consider when developing multi-
562 species biofilms within *in vitro* models. These findings offer valuable insight
563 into understanding the parameters that influence the development of multi-
564 species biofilms within the laboratory.

565

566 **Acknowledgements**

567 The authors thank the donors for their participation in this study. We thank
568 Alexa C. Cannon and Ting L. Luo, University of Michigan, for technical
569 support. This work was supported by the Wm Wrigley Jr. Company. Partial
570 data were presented in 7th ASM Conference on Biofilms, Chicago, USA,
571 2015; 94th IADR General Session & Exhibition, Seoul, South Korea and in the
572 63rd ORCA Congress, Athens, Greece, 2016.

573

574 **Conflict of Interest**

575 The authors declare that the research was conducted in the absence of any
576 commercial or financial relationships that could be construed as a potential
577 conflict of interest. M.W. Dodds and M.B. Aspiras are current employers of
578 the Wm. Wrigley Jr. Company, Chicago, IL, USA.

579

580 **References**

581

582 Aas JA, Paster BJ, Stokes LN, Olsen I & Dewhirst FE (2005) Defining the normal
583 bacterial flora of the oral cavity. *J Clin Microbiol* **43**: 5721-5732.

584 Belstrom D, Holmstrup P, Bardow A, Kokaras A, Fiehn NE & Paster BJ (2016)
585 Comparative analysis of bacterial profiles in unstimulated and stimulated saliva
586 samples. *J Oral Microbiol* **8**: 30112.

587 Brown MR & Gilbert P (1993) Sensitivity of biofilms to antimicrobial agents. *J Appl*
588 *Bacteriol* **74 Suppl**: 87S-97S.

589 Burmolle M, Ren D, Bjarnsholt T & Sorensen SJ (2014) Interactions in multispecies
590 biofilms: do they actually matter? *Trends in Microbiol* **22**: 84-91.

591 Caporaso JG, Bittinger K, Bushman FD, DeSantis TZ, Andersen GL & Knight R
592 (2010a) PyNAST: a flexible tool for aligning sequences to a template alignment.
593 *Bioinformatics* **26**: 266-267.

594 Caporaso JG, Kuczynski J, Stombaugh J, *et al.* (2010b) QIIME allows analysis of
595 high-throughput community sequencing data. *Nat Methods* **7**: 335-336.

596 Ccahuana-Vásquez RA & Cury JA (2010) *S. mutans* biofilm model to evaluate
597 antimicrobial substances and enamel demineralization. *Braz Oral Res* **24**: 135-141.

598 Coenye T & Nelis HJ (2010) In vitro and in vivo model systems to study microbial
599 biofilm formation. *J Microbiol Methods* **83**: 89-105.

600 Collins TJ (2007) ImageJ for microscopy. *BioTechniques* **43**: 25-30.

601 Dawes C, Tsang RW & Suelzle T (2001) The effects of gum chewing, four oral
602 hygiene procedures, and two saliva collection techniques, on the output of bacteria
603 into human whole saliva. *Arch Oral Biol* **46**: 625-632.

604 Dewhirst FE, Chen T, Izard J, *et al.* (2010) The human oral microbiome. *J Bacteriol*
605 **192**: 5002-5017.

606 Fernández CE, Tenuta LM & Cury JA (2016) Validation of a Cariogenic Biofilm Model
607 to Evaluate the Effect of Fluoride on Enamel and Root Dentine Demineralization.
608 *PloS one* **11**: e0146478.

609 Gilbert P, Maira-Litran T, McBain AJ, Rickard AH & Whyte FW (2002) The physiology
610 and collective recalcitrance of microbial biofilm communities. *Adv Microb Physiol*
611 **46**: 202-256.

612 Griffen AL, Beall CJ, Firestone ND, *et al.* (2011) CORE: a phylogenetically-curated
613 16S rDNA database of the core oral microbiome. *PloS one* **6**: e19051.

614 Guggenheim B, Giertsen E, Schupbach P & Shapiro S (2001) Validation of an in
615 vitro biofilm model of supragingival plaque. *J Dent Res* **80**: 363-370.

616 He X, McLean JS, Edlund A, *et al.* (2015) Cultivation of a human-associated TM7
617 phylotype reveals a reduced genome and epibiotic parasitic lifestyle. *Proc. Natl.*
618 *Acad. Sci. U.S.A.* **112**: 244-249.

619 Heydorn A, Nielsen AT, Hentzer M, Sternberg C, Givskov M, Ersboll BK & Molin S
620 (2000) Quantification of biofilm structures by the novel computer program
621 COMSTAT. *Microbiology* **146 (Pt 10)**: 2395-2407.

622 Hojo K, Nagaoka S, Ohshima T & Maeda N (2009) Bacterial interactions in dental
623 biofilm development. *J Dent Res* **88**: 982-990.

624 Jakubovics NS & Kolenbrander PE (2010) The road to ruin: the formation of
625 disease-associated oral biofilms. *Oral Dis* **16**: 729-739.

626 Kim K, Ingremeau F, Zhao A, Bassler B & Stone H (2016) Local and global
627 consequences of flow on bacterial quorum sensing. *Nat Microbiol*
628 doi:10.1038/nmicrobiol.2015.1035.

629 Kinniment SL, Wimpenny JW, Adams D & Marsh PD (1996) The effect of
630 chlorhexidine on defined, mixed culture oral biofilms grown in a novel model
631 system. *J Appl Bacteriol* **81**: 120-125.

632 Kistler JO, Pesaro M & Wade WG (2015) Development and pyrosequencing analysis
633 of an in-vitro oral biofilm model. *BMC Microbiol* **15**: 24.

634 Klapper I, Rupp CJ, Cargo R, Purvedorj B & Stoodley P (2002) Viscoelastic fluid
635 description of bacterial biofilm material properties. *Biotechnol Bioeng* **80**: 289-296.

636 Kolderman E, Bettampadi D, Samarian D, Dowd SE, Foxman B, Jakubovics NS &
637 Rickard AH (2015) L-arginine destabilizes oral multi-species biofilm communities
638 developed in human saliva. *PloS one* **10**: e0121835.

639 Liu Y & Tay JH (2001) Metabolic response of biofilm to shear stress in fixed-film
640 culture. *J Appl Microbiol* **90**: 337-342.

641 Liu Y & Tay JH (2002) The essential role of hydrodynamic shear force in the
642 formation of biofilm and granular sludge. *Water Res* **36**: 1653-1665.

643 Mager DL, Ximenez-Fyvie LA, Haffajee AD & Socransky SS (2003) Distribution of
644 selected bacterial species on intraoral surfaces. *J Clin Periodontol* **30**: 644-654.

645 Mark Welch JL, Rossetti BJ, Rieken CW, Dewhirst FE & Borisy GG (2016)
646 Biogeography of a human oral microbiome at the micron scale. *Proc Natl Acad Sci U*
647 *S A* **113**: E791-800.

648 Marsh PD (2003) Plaque as a biofilm: pharmacological principles of drug delivery
649 and action in the sub- and supragingival environment. *Oral Dis* **9 Suppl 1**: 16-22.

650 Marsh PD (2009) Dental plaque as a biofilm: the significance of pH in health and
651 caries. *Compend Contin Educ Dent* **30**: 76-78, 80, 83-77; quiz 88, 90.

652 McBain AJ (2009) Chapter 4: In vitro biofilm models: an overview. *Adv Appl*
653 *Microbiol* **69**: 99-132.

654 McMurdie PJ & Holmes S (2013) phyloseq: an R package for reproducible interactive
655 analysis and graphics of microbiome census data. *PloS one* **8**: e61217.

656 Nance WC, Dowd SE, Samarian D, Chludzinski J, Delli J, Battista J & Rickard AH
657 (2013) A high-throughput microfluidic dental plaque biofilm system to visualize and
658 quantify the effect of antimicrobials. *J Antimicrob Chemother* **68**: 2550-2560.

659 Netuschil L, Auschill TM, Sculean A & Arweiler NB (2014) Confusion over live/dead
660 stainings for the detection of vital microorganisms in oral biofilms--which stain is
661 suitable? *BMC Oral Health* **14**: 2.

662 Nyvad B & Fejerskov O (1987) Scanning electron microscopy of early microbial
663 colonization of human enamel and root surfaces in vivo. *Scand J Dent Res* **95**: 287-
664 296.

665 Reilly C, Rasmussen K, Selberg T, Stevens J & Jones RS (2014) Biofilm community
666 diversity after exposure to 0.4% stannous fluoride gels. *J Appl Microbiol* **117**:
667 1798-1809.

668 Rickard AH, McBain AJ, Stead AT & Gilbert P (2004) Shear rate moderates
669 community diversity in freshwater biofilms. *Appl Environ Microbiol* **70**: 7426-7435.

670 Rickard AH, Gilbert P, High NJ, Kolenbrander PE & Handley PS (2003) Bacterial
671 coaggregation: an integral process in the development of multi-species biofilms.
672 *Trends Microbiol* **11**: 94-100.

673 Rittman BE (1982) The effect of shear stress on biofilm loss rate. *Biotechnol Bioeng*
674 **24**: 501-506.

675 Rudney JD, Chen R, Lenton P, *et al.* (2012) A reproducible oral microcosm biofilm
676 model for testing dental materials. *J Appl Microbiol* **113**: 1540-1553.

677 Salli KM & Ouwehand AC (2015) The use of in vitro model systems to study dental
678 biofilms associated with caries: a short review. *J Oral Microbiol* **7**: 26149.

679 Samarian DS, Jakubovics NS, Luo TL & Rickard AH (2014) Use of a high-throughput
680 in vitro microfluidic system to develop oral multi-species biofilms. *J Vis Exp*
681 doi:10.3791/52467.

682 Saunders KA & Greenman J (2000) The formation of mixed culture biofilms of oral
683 species along a gradient of shear stress. *J Appl Microbiol* **89**: 564-572.

684 Segata N, Haake SK, Mannon P, *et al.* (2012) Composition of the adult digestive
685 tract bacterial microbiome based on seven mouth surfaces, tonsils, throat and stool
686 samples. *Genome Biol* **13**: R42.

687 Shu M, Morou-Bermudez E, Suarez-Perez E, *et al.* (2007) The relationship between
688 dental caries status and dental plaque urease activity. *Oral Microbiol Immunol* **22**:
689 61-66.

690 Signori C, van de Sande FH, Maske TT, de Oliveira EF & Cenci MS (2016) Influence
691 of the Inoculum Source on the Cariogenicity of in vitro Microcosm Biofilms. *Caries*
692 *Res* **50**: 97-103.

693 Simon-Soro A, Belda-Ferre P, Cabrera-Rubio R, Alcaraz LD & Mira A (2013a) A
694 tissue-dependent hypothesis of dental caries. *Caries Res* **47**: 591-600.

695 Simon-Soro A, Tomas I, Cabrera-Rubio R, Catalan MD, Nyvad B & Mira A (2013b)
696 Microbial geography of the oral cavity. *J Dent Res* **92**: 616-621.

697 Song F, Koo H & Ren D (2015) Effects of Material Properties on Bacterial Adhesion
698 and Biofilm Formation. *J Dent Res* **94**: 1027-1034.

699 Soro V, Dutton LC, Sprague SV, *et al.* (2014) Axenic culture of a candidate division
700 TM7 bacterium from the human oral cavity and biofilm interactions with other oral
701 bacteria. *Appl Environ Microbiol* **80**: 6480-6489.

702 Stoodley P, Cargo R, Rupp CJ, Wilson S & Klapper I (2002) Biofilm material
703 properties as related to shear-induced deformation and detachment phenomena. *J*
704 *Ind Microbiol Biotechnol* **29**: 361-367.

705 ten Cate JM & Zaura E (2012) The numerous microbial species in oral biofilms: how
706 could antibacterial therapy be effective? *Adv Dent Res* **24**: 108-111.

707 Wake N, Asahi Y, Noiri Y, *et al.* (2016) Temporal dynamics of bacterial microbiota in
708 the human oral cavity determined using an in situ model of dental biofilms. *Npj*
709 *Biofilms And Microbiomes* **2**: 16018.

710 Wang Q, Garrity GM, Tiedje JM & Cole JR (2007) Naive Bayesian classifier for rapid
 711 assignment of rRNA sequences into the new bacterial taxonomy. *Appl Environ*
 712 *Microbiol* **73**: 5261-5267.

713 Zaura E, Keijsers BJ, Huse SM & Crielaard W (2009) Defining the healthy "core
 714 microbiome" of oral microbial communities. *BMC microbiology* **9**: 259.

715 Zijngel V, Ammann T, Thurnheer T & Gmur R (2012) Subgingival biofilm structure.
 716 *Front Oral Biol* **15**: 1-16.

717

718

719

720

721

722

723 **Table 1.** Heat map of unweighted UniFrac distances [**average(sd)**]. Shades
 724 of red (lowest values) and blue (largest values) indicate the magnitude of
 725 the differences in community composition between compared groups. Bolded
 726 borders to cells highlight the distances between inoculum and the respective
 727 developed biofilms at 0.1, 0.2 and 0.4 dyn cm⁻² for each inoculum-type.
 728 Statistically significant differences are represented by different letters. The
 729 number of pairwise comparisons was three for within group and nine for
 730 between groups.

		Experimental Groups															
		Saliva				Toothbrush Plaque				Tongue				Curette Plaque			
		Inoc	0.1	0.2	0.4	Inoc	0.1	0.2	0.4	Inoc	0.1	0.2	0.4	Inoc	0.1	0.2	0.4
Saliva	Inoc	.177(.006)^a	.569(.011)	.666(.016)	.591(.009)	.229(.011)	.527(.027)	.570(.021)	.587(.060)	.209(.006)	.518(.029)	.555(.063)	.510(.069)	.301(.008)	.647(.029)	.634(.034)	.684(.026)
	0.1		.329(.026)^b	.419(.032)	.365(.024)	.605(.006)	.373(.012)	.367(.012)	.419(.040)	.575(.017)	.409(.039)	.426(.026)	.419(.030)	.650(.005)	.459(.032)	.424(.018)	.468(.071)
	0.2			.393(.043)^b	.412(.025)	.691(.014)	.470(.046)	.423(.024)	.469(.035)	.666(.015)	.480(.037)	.447(.045)	.489(.053)	.712(.013)	.470(.024)	.433(.029)	.461(.059)
	0.4				.399(.006)^c	.631(.006)	.420(.030)	.402(.023)	.439(.045)	.596(.010)	.419(.032)	.417(.021)	.426(.032)	.659(.008)	.470(.026)	.441(.024)	.485(.060)
Toothbrush Plaque	Inoc					.158(.020)^a	.552(.021)	.594(.018)	.609(.061)	.277(.011)	.563(.025)	.600(.051)	.558(.060)	.191(.006)	.660(.028)	.652(.034)	.700(.027)
	0.1						.314(.018)^b	.345(.034)	.375(.065)	.557(.020)	.433(.027)	.475(.016)	.449(.028)	.584(.017)	.448(.028)	.415(.023)	.477(.067)

753 **Figure 5.** Principal coordinate analysis (PCoA) plot is based on community
754 variation using Unifrac distance. The figure represents original inocula (A)
755 [blue (curette-plaque), purple (toothbrush-plaque), red (saliva) and green
756 (tongue)] and the respective developed biofilms (B) grown at three different
757 fluid shear force levels. Color-scale of blue (curette-plaque), purple
758 (toothbrush-plaque), red (saliva) and green (tongue) represent the
759 developed biofilms grown at 0.1, 0.2 or 0.4 dyn cm⁻². Circle lines represent
760 clustering by inoculum type.

761

762 **Table S1.** Quantification of biofilm architecture of developed biofilms
763 (**average** (SD): n= 16 per group).

764

765 **Figure S1.** Relative abundance by genus composition (n=3 samples per
766 group). Each original inoculum and the respective developed-biofilms grown
767 at fluid shears of 0.1, 0.2 or 0.4 dyn cm⁻² are represented by inoculum type.

Author Manuscript

Developed Biofilms

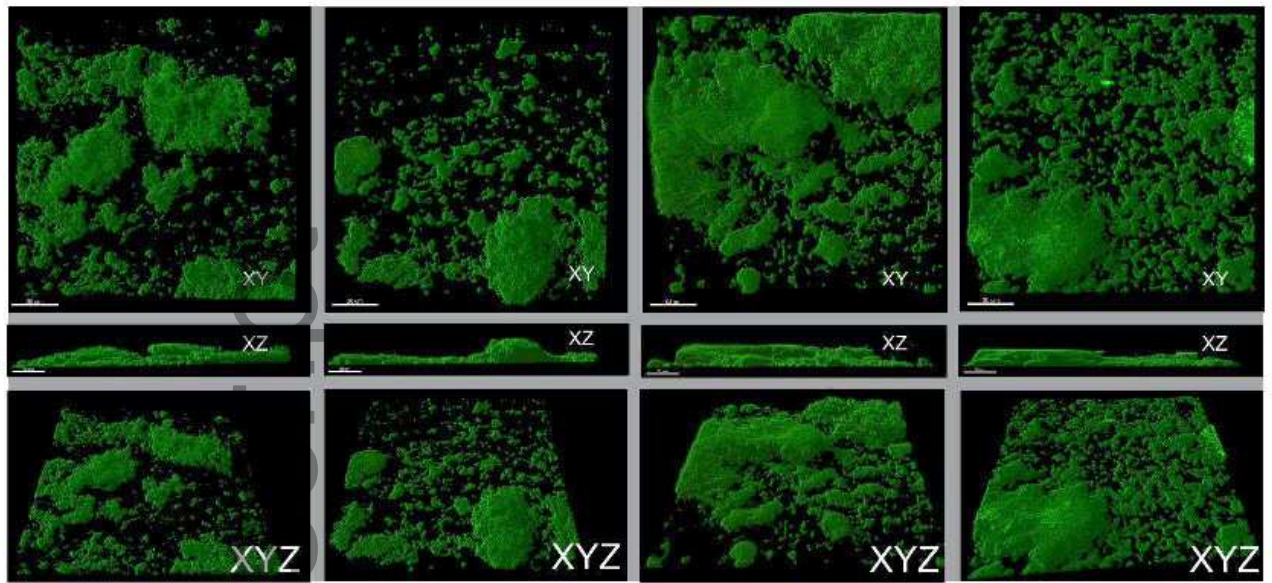
Saliva

Tongue

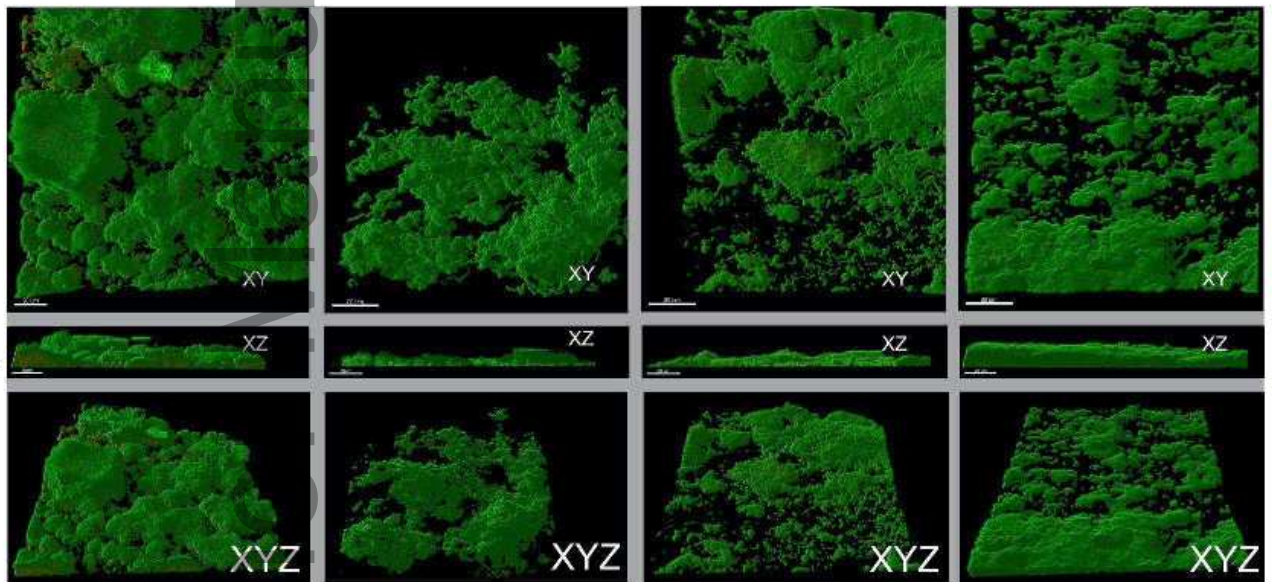
Toothbrush plaque

Curette plaque

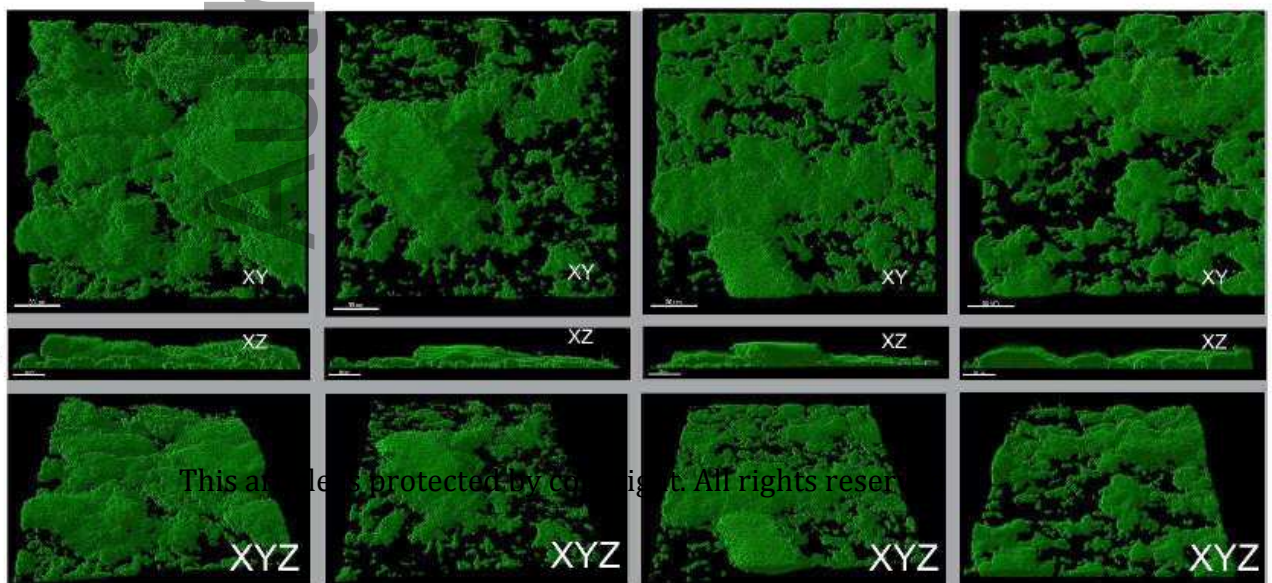
0.1 dyn cm⁻²



0.2 dyn cm⁻²



0.4 dyn cm⁻²



This article is protected by copyright. All rights reserved.

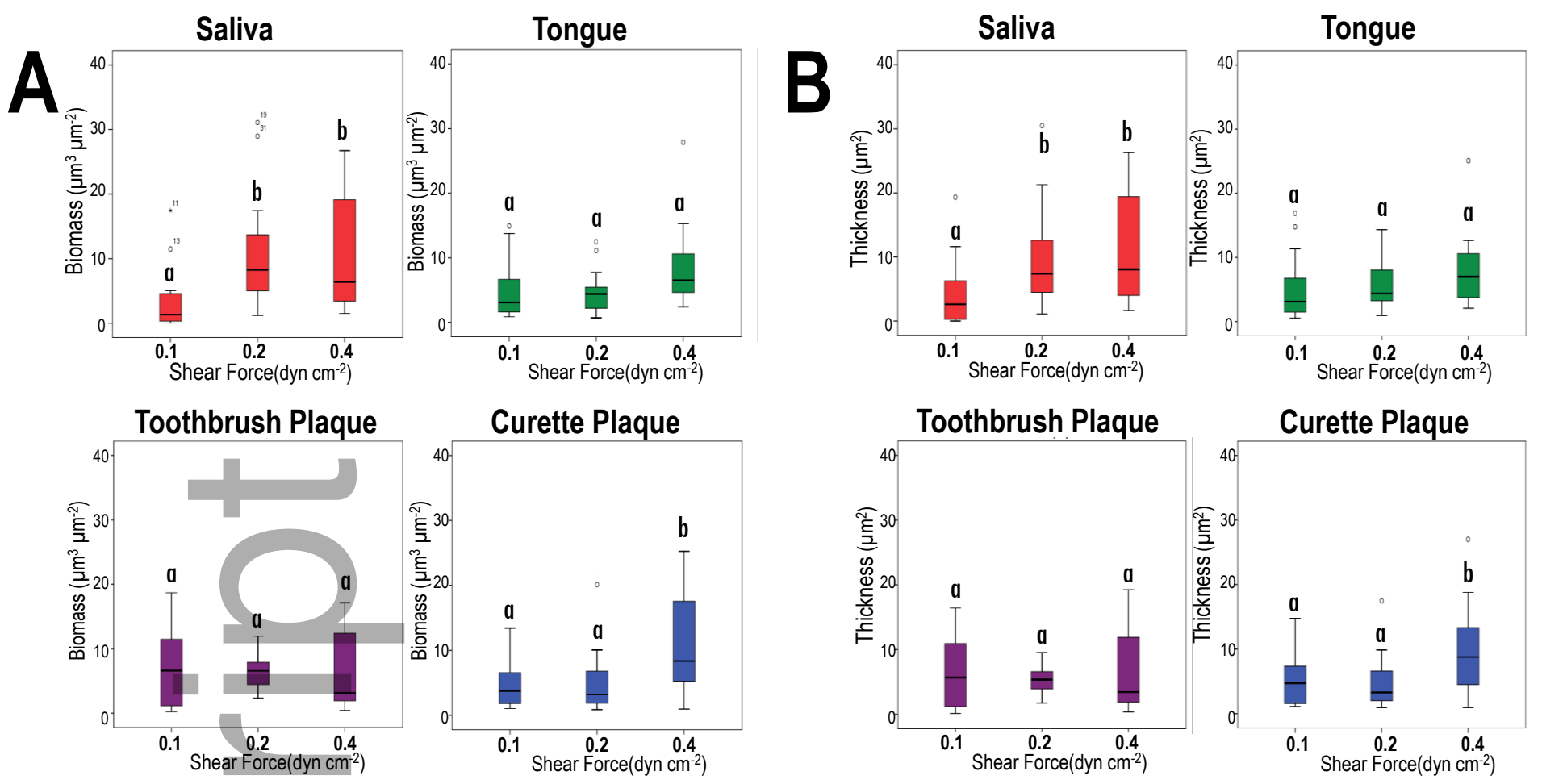


Fig 2

Author Manuscript

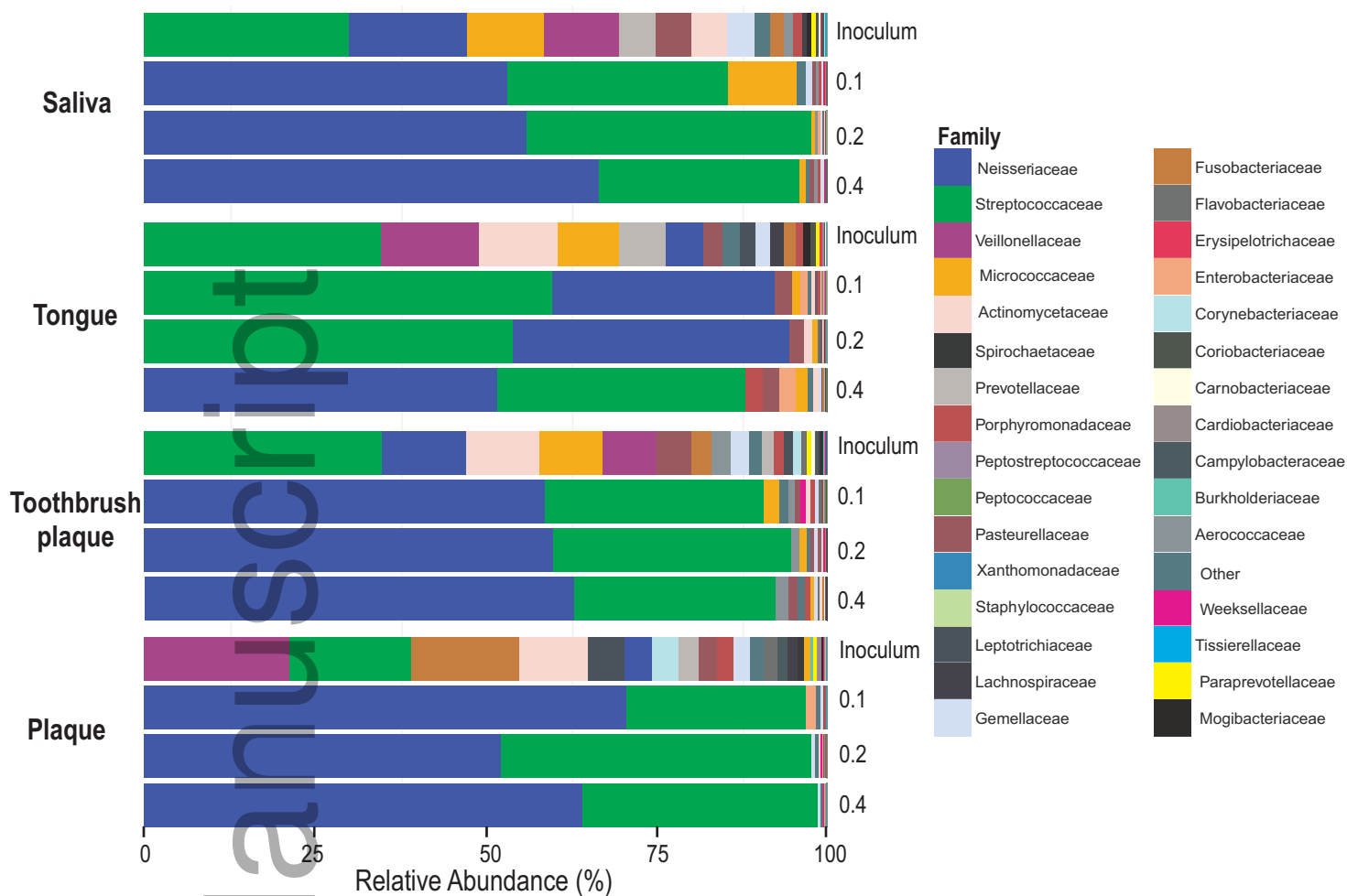


Fig 3

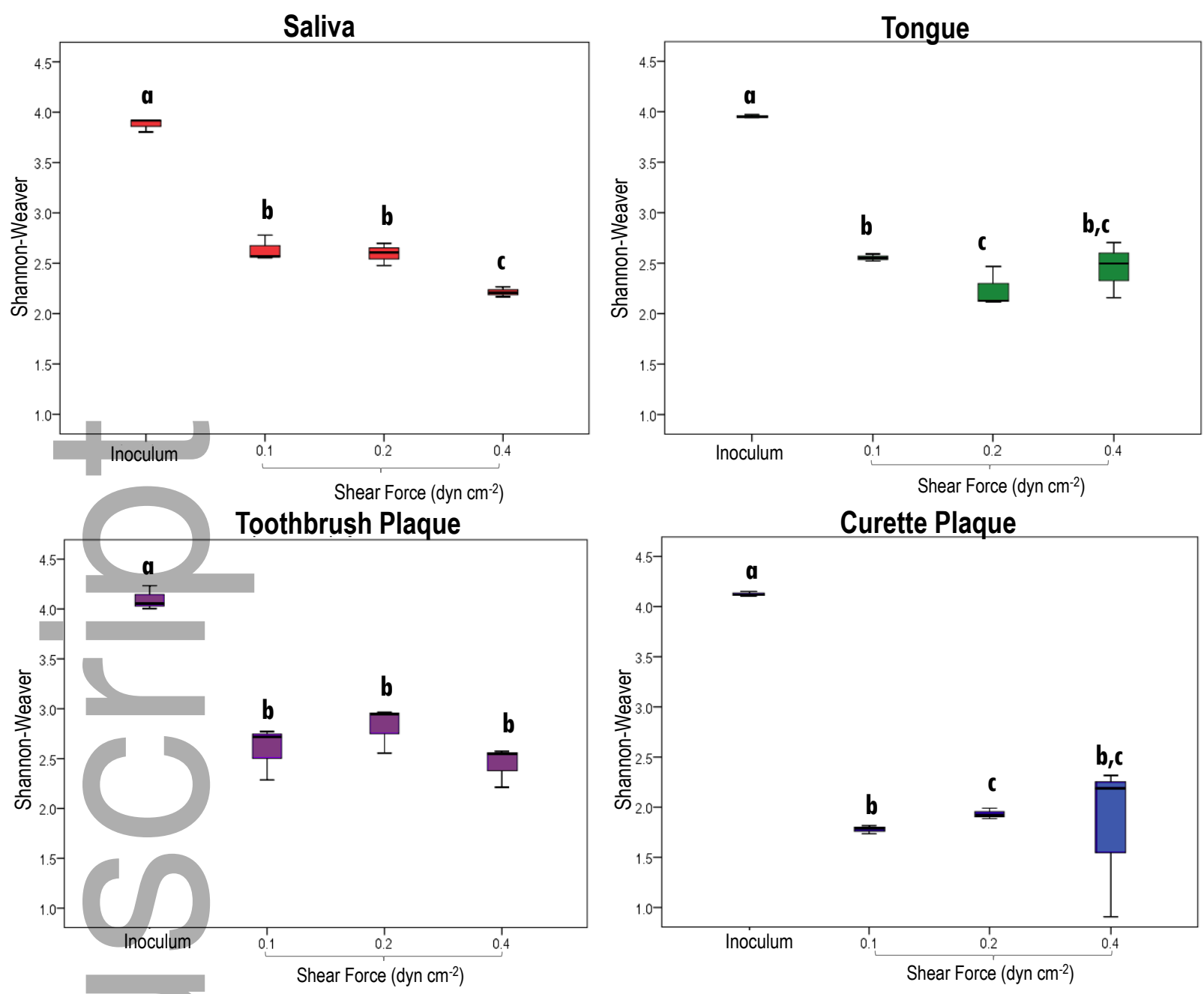


Fig 4

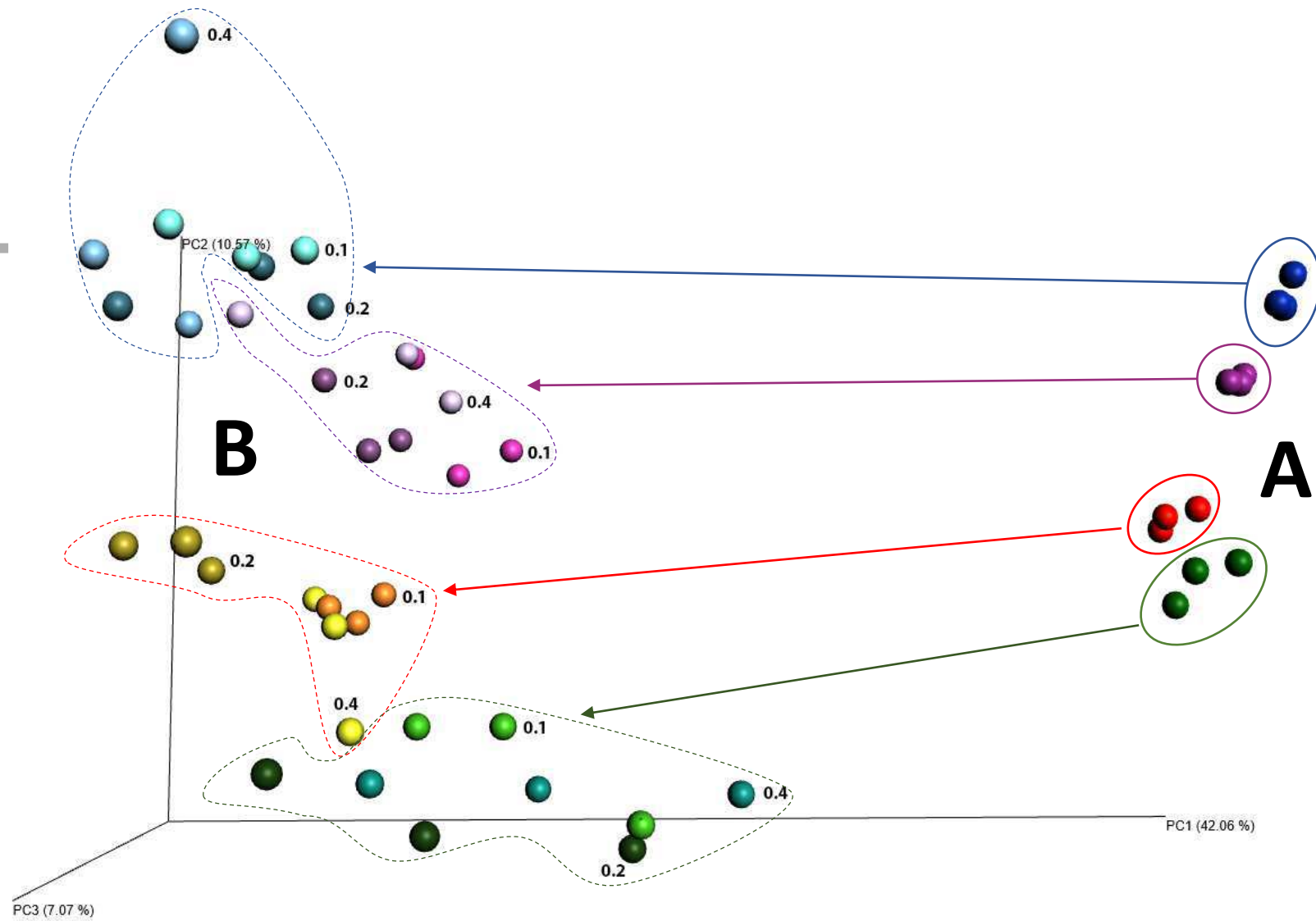


Fig 5